Antiviral Research 93 (2012) 288–296

Contents lists available at SciVerse ScienceDirect

Antiviral Research

journal homepage: www.elsevier.com/locate/antiviral

In vitro resistance selections using elvitegravir, raltegravir, and two metabolites of elvitegravir M1 and M4

Nicolas A. Margot *, Rebecca M. Hluhanich, Gregg S. Jones, Kristen N. Andreatta, Manuel Tsiang, Damian J. McColl, Kirsten L. White, Michael D. Miller

Gilead Sciences, Inc., 333 Lakeside Drive, Foster City, CA 94404, USA

ARTICLE INFO

Article history:
Received 27 August 2011
Revised 8 December 2011
Accepted 9 December 2011
Available online 16 December 2011

Keywords:
HIV
Integrase inhibitor
Resistance selection

ABSTRACT

Elvitegravir is a strand transfer inhibitor of HIV-1 integrase that is currently undergoing phase 3 clinical testing. The two predominant metabolites of elvitegravir, M1 and M4 (elvitegravir hydroxide and elvitegravir glucuronide), have been shown to inhibit HIV-1 integrase in vitro. While they are markedly less potent than elvitegravir and present only at low levels in plasma clinically, we investigated their potential to select for elvitegravir resistance in vitro. Resistance selection experiments using metabolites M1 and M4 led to the development of the previously reported elvitegravir integrase resistance mutations H51Y, T66A, E92G, and S147G, as well as a novel S153F substitution. Additional resistance selection experiments using elvitegravir led to the development of previously reported integrase inhibitor resistance mutations (T66I, F121Y, and S153Y) as well as a novel R263K integrase mutation. Phenotypic analyses of site-directed mutants with these mutations demonstrated broad cross-resistance between elvitegravir and its M1 and M4 metabolites with more limited cross-resistance to the integrase inhibitor raltegravir. Overall, our in vitro studies demonstrate that the resistance profile of the M1 and M4 metabolites of elvitegravir overlaps with that of the parent molecule elvitegravir; as such, their presence at low levels is not considered clinically relevant.

1. Introduction

The outcome of HIV-1 infection has been greatly improved during the last decade, primarily due to advances in the therapeutic options that are now available to HIV-1-infected patients and the physicians who treat them. However, development of viral resistance to existing therapies remains a critical issue in the management of long-term HIV infection (Johnson et al., 2010), underlining the need to develop new ways of controlling HIV-1 replication in patients who develop resistance. Such new approaches have been to focus therapeutic research on attacking new targets of the HIV viral lifecycle such as viral fusion and entry into CD4 positive target cells (Dorr et al., 2005; Kilby et al., 1998), that has led to FDA approval of enfuvirtide (T-20) in 2003 and maraviroc in 2007 for the treatment of HIV-1 infection in combination with other agents.

Another novel approach to combat HIV-1 infection has focused on the step of HIV-1 genome integration into the host cell DNA, which is accomplished through the action of the virally encoded HIV-1 integrase enzyme (reviewed in Marchand et al., 2009; Pommier et al., 2005) in concert with cellular factors such as LEDGF (Cherepanov et al., 2005, 2003; Maertens et al., 2003) and components of the host DNA repair machinery (Yoder and Bushman, 2000; Yoder et al., 2011). The integration process involves several steps that includes 3′-processing of the viral cDNA, pre-integration complex formation, transfer into the nucleus, viral cDNA strand transfer into the host chromosomal DNA, and DNA gap repair. In 2007 raltegravir was the first integrase strand transfer inhibitor (INSTI) to gain approval by the FDA for the treatment of HIV-1 infection in combination with other agents. Two other INSTIs, elvitegravir (GS-9137/JTK-303) (Molina et al., 2011) and dolutegravir (S/GSK1349572) (van Lunzen et al., 2011) are currently under clinical development. All three compounds inhibit the HIV-1 integrase strand transfer reaction with nanomolar activity (Kobayashi et al., 2011; Marinello et al., 2008; Shimura and Kodama, 2009).

Virologic failure during raltegravir treatment in vivo has been associated primarily with the integrase mutations N155H, E92Q, Q148R/H/K, G140S/A, and Y143C (Cooper et al., 2008; Fransen et al., 2009) which confer a loss of raltegravir susceptibility ranging from 6-fold to >150-fold of wild-type as well as cross-resistance to elvitegravir and other INSTIs in most cases. The mutation E157Q was also associated with raltegravir treatment failure (Malet et al., 2008). In vitro resistance selection experiments with elvitegravir have led to resistant viruses containing the mutations T66I, Q95K, E138K, Q146P, and S147G in one instance; and H51Y, E92Q, S147G, and E157Q in a second set of experiments (Shimura et al.,

* Corresponding author. Tel.: +1 650 522 5445; fax: +1 650 522 5890.
E-mail address: Nicolas.Margot@gilead.com (N.A. Margot).

0166-3542/$ - see front matter © 2011 Elsevier B.V. All rights reserved.
doi:10.1016/j.antiviral.2011.12.008

2008). Viruses containing these mutations were associated with high-level resistance to elvitegravir. Another virus containing the mutations H114Y, A128T, and Q148R was also reported to exhibit resistance to a broad range of INSTIs (Goethals et al., 2008).

Elvitegravir is primarily metabolized in vitro by cytochrome P450 as well as by uridine glucuronosyltransferase 1A1/3 to yield the metabolites M1 (elvitegravir hydroxide) and M4 (elvitegravir glucuronide), respectively (Fig. 1) (Ramanathan et al., 2007). When co-administered with ritonavir, plasma exposures of these anti-HIV-1 active metabolites only represent a small fraction of the total elvitegravir species (M1: 2.5%; M4: 1%), and are not thought to play a significant role in the overall antiviral activity of elvitegravir since they also exhibit lower potency than the predominant elvitegravir (Ramanathan et al., 2007).

In the study presented here we have conducted a series of resistance selection experiments aimed at characterizing the in vitro resistance profile of the two predominant metabolites of elvitegravir, M1 and M4, and we have investigated in more detail the in vitro resistance profile of elvitegravir and raltegravir using two different resistance selection approaches.

2. Materials and methods

2.1. Reagents and cell lines

Elvitegravir (EVG), raltegravir (RAL), efavirenz (EFV), and tenofovir (TFV) were synthesized at Gilead Sciences (Foster City, California). The metabolites M1 and M4 were supplied by Japan Tobacco (Osaka, Japan). MT-2 cells were obtained from the National Institutes of Health AIDS Research and Reference Reagent Program (Germantown, MD). SUP-T1 and HEK293T cells were purchased from American Type Culture Collection (ATCC; Manassas, VA). Wild-type virus stocks HIV-1_{IIIB} and HIV-1_{HXB2D} were purchased from Advanced Biotechnologies Inc., (Columbia, MD).

2.2. Selection conditions

Dose escalation single compound resistance selection experiments using EVG (two separate experiments), RAL, M1, and M4 were performed. Additionally, viral breakthrough resistance selection experiments using the clinical compounds EVG and RAL were conducted.

For the dose escalation method, experiments were set up in 6-well plates with 0.5 million MT-2 cells per well in a final volume of 5 ml. At the start of the experiment, cells were infected with 5 μl of a 1:200 dilution of HIV-1_{IIIB} viral stock corresponding to a multiplicity of infection (MOI) around 0.01. The starting concentrations of compounds used were set to correspond to either 1-fold or 2-fold the EC_{50} of the compounds depending on the experiments. As the experiments were conducted over a period of several years, minor fluctuations in the EC_{50}s for each of the compounds over time have resulted in slight deviations in the fold EC_{50} that was used when re-calculated using the latest EC_{50} values for the various compounds. As a result, the intended 1-fold EC_{50} EVG concentration in the first EVG experiment was slightly below the current EC_{50} (0.4 nM compared to the current HIV-1_{IIIB} EVG EC_{50} of 0.6 nM), and the intended 2-fold EC_{50} EVG concentration in the second experiment was slightly above 2-fold the current EC_{50} (1.5 nM compared to 1.2 nM). Different starting EVG concentrations were used in these two experiments in order to study the effect of the initial selective pressure on the resulting viral population. The RAL selection experiment was conducted in parallel with the second EVG experiment and the intended 2-fold EC_{50} RAL concentration was slightly below 2-fold the current EC_{50} (5 nM compared to the current RAL EC_{50} of 3 nM for HIV-1_{IIIB}). For similar reasons, the intended 2-fold EC_{50} starting concentrations of M1 and M4 were about 4-fold above the current EC_{50}s for these two compounds (20 and 17 nM compared to HIV-1_{IIIB} EC_{50} of 5.6 and 4 nM for M1 and M4, respectively). One well without drug was used as an infection control. The cultures were incubated at 37 °C and split 1:2 once or twice weekly depending on the growth status of the cells. Under these culture conditions, 50% of infected cells were discarded during each split to prevent overgrowth of the culture. Cytopathic effect (CPE), in the form of cellular syncytia in the no-drug culture, was observed approximately 4 days after initiation of infection. When extensive CPE was seen in the drug wells, viral supernatants were harvested and a new passage was generated by infecting fresh MT-2 cells with 5–50 μl of the harvested virus using a drug concentration 2-fold higher than in the previous passage. One well containing no drug as well as one well maintained at the previous drug concentration were also set up as controls for viral growth. Successive viral passages were obtained by repeating this procedure. The duration of each passage at a given drug concentration was dependent upon the development of CPE in the drug wells and ranged from 5 to 27 days. Viral supernatants were prepared and sequenced (population sequencing, and clonal sequencing on select samples) as described below.

For the viral breakthrough selections, 2 million SUP-T1 cells were infected with HIV-1_{HXB2D} at an MOI of 0.1 in a total volume of 4 ml in 6-well plates and cultured in the presence of constant drug concentration over time. The drug concentrations used in these experiments were 5-, 10-, 20-, 40-, and 80-fold above the EC_{50} for EVG and RAL, and were 10-, 20-, 40-, 80-, and 160-fold above the EC_{50} for EFV, which was used as a control. One well containing no drug was set up as an infection control. After a week in culture, viral supernatants were harvested when CPE was observed and cells were split 1:6 and put back in culture in the presence of fresh drug. Fresh SUP-T1 cells (1 million) were added when complete cell killing was observed. Control wells containing no drug were set up at each passage. The cultures were maintained for up to 45 days, and the last viral supernatants obtained were prepared and sequenced (population sequencing) as described below.

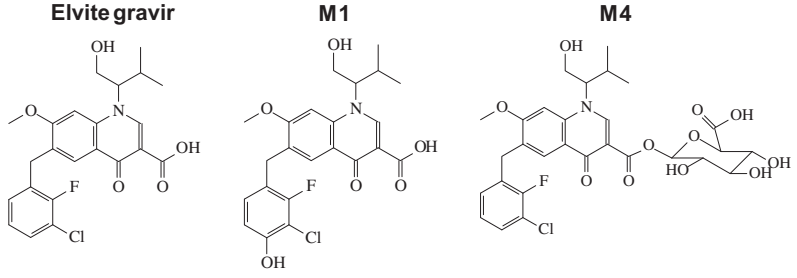

Fig. 1. Structure of elvitegravir and its metabolites M1 and M4. M1 (elvitegravir hydroxide) results from the metabolism of elvitegravir by cytochrome P450 3A (CYP3A4), and M4 results from the metabolism of elvitegravir by uridine glucuronosyltransferase 1A1/3 (UGT1A1/3).

2.3. Sample preparation and sequencing

Viral supernatant (140 μl) was DNase treated (DNase I; New England Biolabs, Ipswich MA) at room temperature for 45 min in the presence of magnesium, and viral RNA was extracted using a QIAamp Viral RNA kit (QIAGEN, Valencia, CA) and eluted in 75 μl of water. Viral cDNA was generated using Ready-To-Go™ You-Prime First-Strand cDNA kit (GE Healthcare, Buckinghamshire, UK) using the 3′ primer, pLAIR5768 (5′-CTAAGCCATGGAGCCA AATCC-3′). For population sequencing, 5 μl of viral cDNA was used to amplify a 2765 base pair viral DNA fragment spanning nucleotide 372 of the RT gene to nucleotide 127 of the Vpr gene by polymerase chain reaction (PCR). The primers used for PCR were pLAIF3004 (5′-CAGGAAGTATACTGCATTTACC-3′) and pLAIR5768, and the PCR reaction was performed using Pfu Ultra II Fusion HS DNA polymerase (Stratagene, La Jolla, CA) in a PTC-200 Thermal Cycler (MJ Research, Waltham, MA). The PCR product was purified using the QIAquick PCR purification kit (QIAGEN) and sequenced through the integrase region on both DNA strands (ELIM Biopharmaceuticals Inc., Hayward, CA).

2.4. Clonal sequencing

Viral cDNA was amplified by PCR to generate a 1296 base pair viral DNA fragment spanning nucleotide 1608 of the RT gene to nucleotide 412 of the Vif gene using the primers INTseq14157 (5′-ACCAGCACACAAAGGAATTGG-3′) and VIFseq2Rev5453 (5′-CCT GCTTGATATTCACACC-3′). The PCR product was purified on a 1.0% agarose gel and cloned using the Zero-Blunt-TOPO PCR cloning kit (Invitrogen, Carlsbad, CA). Thirty transformed bacterial colonies were isolated and cultured overnight at 37 °C in LB medium containing 50 μg/mL kanamycin. Plasmid DNAs were isolated using a Wizard SV 96 plasmid purification kit (Promega, Madison, WI) and sequenced through the integrase region on both DNA strands (ELIM Biopharmaceuticals, Inc.).

2.5. Construction of site-directed plasmids and viruses

Mutations of interest were introduced into the infectious wild-type HIV-1 DNA clone pHXB2D by site-directed mutagenesis (Stratagene, La Jolla, CA). The 15.5 Kb pHXB2D plasmid DNA was cut with ApaI and SalI (New England Biolabs) to generate a 3.7 Kb ApaI–SalI fragment that was gel-purified. This 3.7 Kb fragment containing both the RT and the IN genes was then subcloned into pUNI/V5-His B (Invitrogen) to generate pHXB2(3.7). Mutations were selectively introduced into integrase using the Quickchange Site-Directed Mutagenesis Kit (Stratagene) to generate the mutated clones, pHXB2(3.7)mut. After sequence confirmation, pHXB2(3.7)mut plasmid DNA clones were prepared (Qiagen) and the ApaI–SalI fragment containing the integrase mutation(s) was isolated and subcloned back into pHXB2D by replacement of the wild-type 3.7 Kb ApaI–SalI fragment. The 11.8 Kb SalI–ApaI vector fragment necessary for this subcloning steps was prepared by complete digestion of pHXB2D with ApaI (cuts once in pHXB2D), followed by partial digestion with SalI (cuts twice in pHXB2D). The resulting partial digest of pHXB2D was separated by agarose gel electrophoresis and the 11.8 Kb vector fragment was isolated.

TransIT-LT1 (Mirus Bio Corporation, Madison, WI, USA) was used to transfect 7 μg of the viral plasmid DNA (polyclonal or clonal) in 2 million 293T cells seeded in T-25 cell culture flasks in a 6-ml volume 1 day before transfection. The cell culture supernatant containing the virus stock was harvested 2 days after transfection and monitored by p24 assay (Beckman Coulter, Fullerton, CA) and phenotypic assays.

2.6. Phenotyping assay

The phenotype of selected viral pools of interest as well as site directed mutants viruses was determined using a 5-day antiviral assay in MT-2 cells with luciferase readout (CellTiterGlo; Promega). MT-2 cells (1.2 million) were incubated with virus for 3 h at 37 °C in 1 ml screw-cap tubes. The amount of virus used was normalized to yield a signal-to-noise ratio (uninfected cells to infected cells) in the range of 4–7, which was equivalent to an MOI around 0.003 for wild-type HIV-1_{IIIB}. Threefold dilutions of the drugs of interest were prepared in triplicate directly in the eight middle columns of the 96-well assay plates in culture medium containing DMSO at a final concentration of 1%. Column 2 of the assay plates contained no drug and was reserved for the uninfected cell control, while column 11 was reserved for the infected cell control, also without drug. After the 3 h incubation, the infected MT-2 cells and uninfected cell control were diluted 1:7 to a concentration of 0.17 million/ml with tissue culture medium and 100 μl of cell suspension was transferred in triplicate to the appropriate wells in the assay plates. The assay plates were incubated for 5 days at 37 °C. After 5 days, 100 μl of supernatant was removed from each well and 100 μl of CellTiterGlo reagent was added. Plates were incubated at room temperature for 10 min and luminescence was measured using a Wallac Victor2 luminometer (Perkin–Elmer, Shelton, CT).

2.7. Data analysis

For the phenotyping assays, percent cell death in the drug-containing wells in comparison to the uninfected cell control was calculated using Excel (Microsoft, Redmond, WA), and the data were plotted using SigmaPlot (SPSS, Chicago, IL). The effective concentration to inhibit 50% of viral replication (EC_{50}) was also determined using SigmaPlot. Sequencing data were analyzed using SeqMan and MegAlign (DNAStar, Madison, WI). Statistical significance of the fold changes for the mutants compared to the wild-type control was calculated using Excel (*t*-test).

3. Results

3.1. Resistance selections with M1 and M4

The M1 and M4 metabolites of EVG were studied in resistance selection experiments in order to investigate their potential impact on the development of resistance to EVG. The dose escalation method was used to conduct these experiments, and the effect of the increasing selective pressure on the wild-type HIV-1_{IIIB} from these compounds was assessed by analyzing the genotypic and phenotypic changes in the virus over time. The time course of the selection and the genotypic changes for each of the metabolites are shown in Fig. 2 (panels A and B for M1, panels C and D for M4) and summarized in Table 1. For metabolite M1, the primary integrase mutation was H51Y which was first detected as a mixture with wild-type at passage 2, and was detected as a full mutant starting at passage 4. Clonal sequencing analyses of the viral pools (Fig. 2B) have shown that by passage 8 nearly 100% of the clones contained the H51Y mutation, and phenotypic analyses of the viral pools collected at passage 8 detected a 32-fold decrease in susceptibility to M1 compared with wild-type as well as some cross-resistance to EVG (3.5-fold compared to wild-type; Table 2). By passage 11, the selected virus had acquired the four additional mutations D10E, S17N, S147G, and V281M on top of the existing H51Y, and nearly all the clones tested contained all five mutations. Addition of these mutations to the H51Y mutant in the selected virus at passage 10 led to a further 10- and 8-fold decrease in phenotypic susceptibility to M1 and EVG, respectively, when compared to passage 8 (Table 2). Clonal sequencing analysis of selected viral pools

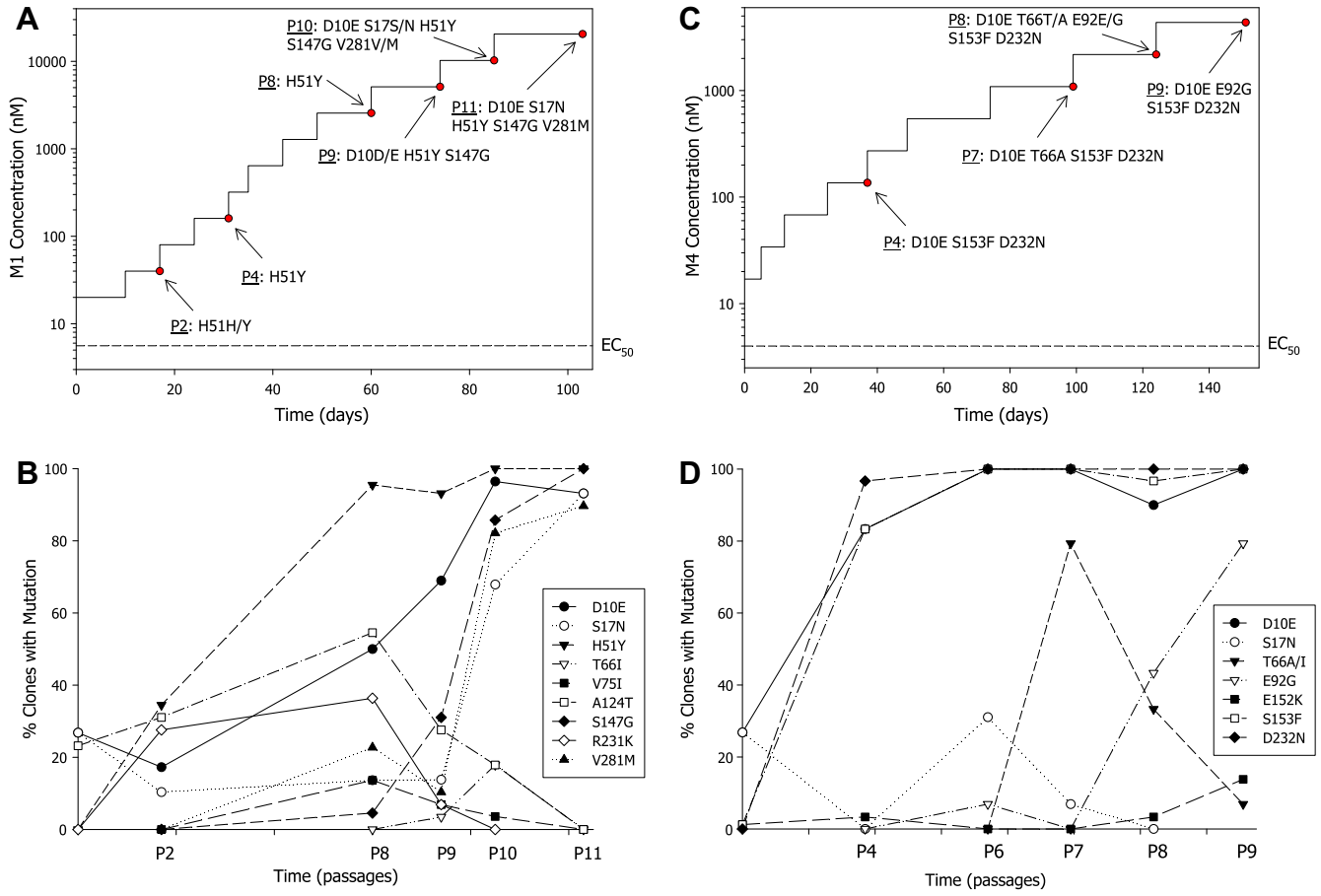

Fig. 2. HIV-1 selection time courses using the EVG metabolite M1 (panel A), and using the EVG metabolite M4 (panel C). Clonal sequencing analysis of the selected viral pools (24–30 clones per timepoint) is shown underneath the selection time course for each of the selections (panel B, clonal sequencing from M1 selection; panel D, clonal sequencing from M4 selection). Amino acid changes compared to HIV-1_{IIIB} starting material (time 0) are plotted.

Table 1
Endpoint summary from the dose escalation selections.

Selecting compound	Final drug concentration (nM)	Fold over EC_{50}[a]	Selection duration (days)	Final integrase amino acid sequence[b]
M1	20480	2048	103	D10E S17N H51Y S147G V281M
M4	4352	512	151	D10E E92G S153F D232N
EVG #1	1640	2730	171	D10E S17N T66I R263K
EVG #2	3072	5120	121	D10E S17N T66I F121F/Y S153S/Y[c] D232N
RAL	5120	1024	132	Q148R D232N

M1, metabolite 1; M4, metabolite 4; EVG, elvitegravir; RAL, raltegravir.
[a] Wild-type HIV-1_{IIIB} EC_{50} values for the selecting compounds were 5.6, 4, 0.6, and 3 nM for M1, M4, EVG, and RAL, respectively.
[b] The selected viruses were sequenced (population sequencing) and compared to HIV-1_{LAI} consensus.
[c] The S153Y mutation was not detected by population sequencing but was present in 50% of the clones in the clonal sequencing analysis.

demonstrated the presence of the two mutations V75I and R231K, which were observed transiently during the course of the selection with M1 and disappeared by passage 10. The T66I mutation was also observed transiently from passage 9 to passage 10 but was not detected by passage 11. The baseline polymorphism A124T was detected in >50% of clones at passage 8 and became undetectable by passage 11.

Resistance selection to the metabolite M4 (Fig. 2, panels C and D) was characterized by the S153F mutation which was first detected as early as passage 4; it was followed by the transient addition of the mutation T66A at passage 7 which decreased and was replaced by the E92G mutation by passage 9. Clonal analyses (Fig. 2D) showed that while the T66A/I mutation decreased from 79% to 33% to 7% of the clones at passage 7, 8, and 9, respectively, the E92G mutation increased from 0% to 43% to 79% of the clones. Most clones were mutually exclusive for E92G and T66A/I, however, one clone containing both T66A and E92G was found at passage 8 and passage 9. A mutation at position 152 (E152K), which was found in 1/82 of the wild-type HIV-1_{IIIB} clones was found in 1/30 clones at passage 4 and passage 8, and was found in 4/29 clones by passage 9. All of these genotypic changes occurred in the background of the D10E and D232N mutations. Phenotypic analyses showed similar decreases in susceptibility to M4 and EVG for the selected pools (Table 2). At passage 4, which harbored the S153F mutation, low-level reduced susceptibility to M4 and EVG was measured at 5.5- to 7.3-fold above wild-type, respectively. Upon addition of the T66A mutation at passage 7, the loss of susceptibility to both M4 and EVG increased to nearly 60-fold

Table 2
Phenotypic susceptibilities of selected viral supernatants from dose escalation selections.

Selecting compound	Passage	Integrase amino acid sequence[a]	EC_{50} fold change compared to wild type[b,c]				
			M1	M4	EVG	RAL	TFV
M1	P2	H51H/Y	2.3	–	1.1	–	–
	P8	H51Y	32	–	3.5	–	–
	P10	D10E S17S/N H51Y S147G V281V/M	326	–	28	–	–
M4	P4	D10E S153F D232N	–	5.5	7.3	2.1	1.2
	P7	D10E T66A S153F D232N	–	59.8	56.1	2.3	1.0
	P8	D10E T66T/A E92E/G S153F D232N	–	79.5	90.2	3.7	1.4
	P9	D10E E92G S153F D232N	–	115	93.1	4.0	1.3
EVG #2	P3	T66T/I	–	–	7.8	0.9	0.9
	P6	T66I D232D/N	–	–	41.9	3.0	1.0
	P12	D10E S17N T66I F121F/Y S153S/Y[d] D232N	–	–	585	–	0.9

M1, metabolite 1; M4, metabolite 4; EVG, elvitegravir; RAL, raltegravir; TFV, tenofovir; '–', not determined.
[a] The selected viruses were sequenced and compared to HIV-1_{LAI} consensus.
[b] Wild-Type HIV-1_{IIIB} EC_{50} values were 4, 5.6, 0.6, 3 nM, and 3.4 μM for M4, M1, EVG, RAL, and TFV, respectively.
[c] Fold change values ⩽2.5 reflect assay variation. All fold change values >2.5-fold demonstrated a statistically significant difference compared to wild-type using the student *t*-test ($p < 0.01$).
[d] The S153Y mutation was not detected by population sequencing but was present in 50% of the clones in the clonal sequencing analysis.

above wild-type, and reached 115- and 93-fold of wild-type for M4 and EVG, respectively, at passage 9 when the selected virus predominantly expressed the E92G mutation in addition to the S153F mutation.

3.2. Elvitegravir and raltegravir selections

Two methods were used to assess the development of resistance mutations to EVG and RAL in vitro. The first method utilized dose-escalation where the drug concentration was increased 2-fold from one passage to the next when viral replication was detected based on observed cytopathic effect. The second method utilized breakthrough selection where infected cells were subjected to drug selective pressure at constant drug concentrations throughout the culture period. Two independent selection experiments using the dose escalation method were performed for EVG and their time courses are shown in Fig. 3, panels A and C. In the first experiment the selection started near the EC_{50} for EVG while in the second experiment the selection started at an EVG concentration of 2.5 times the EC_{50}. Both experiments led to the development of resistant viruses that carried the primary EVG resistance mutation T66I. In the first experiment, an R263K mutation developed at the end of passaging, and both T66I and R263K were present in the background of D10E, and S17N. Clonal sequencing analyses (Fig. 3B) showed that the three mutations D10E, S17N, and T66I were present in almost 100% of the clones by passage 8, while a G163R mutation was observed transiently in 3/24 clones. The R263K mutation increased from 1/24 clones at passage 8 to 100% of the clones by passage 11.

In the second EVG selection experiment (Fig. 3C), D232N was first added to T66I and was followed by the addition of a transient S153Y mutation that was replaced by an F121Y mutation by the end of the experiment, while the selected virus was also showing the addition of the D10E and S17N mutations. Clonal sequencing analyses (Fig. 3D) showed that the S153Y mutation was present in about 50% of the clones from passage 9 until the end of the experiment when it was not detected by population sequencing. The F121Y mutation was found in >20% of the clones from passage 6 to passage 9 when it was not detected by population sequencing, and was present in >50% of the clones by passage 12. The F121Y mutation became gradually associated with the T66I mutation (4/30 clones, 7/28 clones, and 15/28 clones at passage 6, passage 9, and passage 12, respectively), and was rarely found on the same genome with the S153Y mutation (2/28 clones, and 1/28 clones, at passage 9 and passage 12, respectively, in the presence of T66I). The S153Y mutation appeared evenly associated with T66I from passage 9 to passage 12 (15/28 clones and 14/28 clones, respectively). Presence of the T66I mutation at passage 6 was associated with a nearly 42-fold reduced susceptibility to EVG when compared to the wild-type (Table 2), and the addition of the F121Y and S153Y mutations on top of T66I at passage 12 further increased the resistance of the selected virus pool to nearly 600-fold of wild-type. A G82E mutation was identified in 3/28 clones by passage 12, with 1 clone associated with F121Y and 2 clones associated with S153Y.

Resistance selection using the reference compound RAL led to a virus containing the Q148R characteristic RAL mutation and the D232N mutation at passage 11 (Table 1; final RAL concentration of 5120 nM, 1024-fold above EC_{50}). The development of integrase resistance appeared with similar kinetics in both the EVG and the RAL resistance selection experiments (data not shown).

For the breakthrough selection method, selection experiments were started with a high amount of virus (MOI of 0.1) and used constant drug concentrations throughout the experiment. Five different drug concentrations corresponding to 5-, 10-, 20-, 40-, and 80-fold the EC_{50} for EVG and RAL were used in these experiments (Table 3). Viral breakthrough selections with the non-nucleoside RT inhibitor control compound efavirenz (EFV) led to viruses containing the mutation L100I in RT in combination with the D237N RT mutation (at 10- and 20-fold over EC_{50}) or the V108I RT mutation (at 80-fold over EC_{50}). Viral breakthrough was also observed among the five drug concentrations tested in the EVG and RAL experiments (Table 3). Resistant virus was observed at an EVG concentration corresponding to 10-fold the EC_{50} (T66I/T), and 40- and 80-fold the EC_{50} (Q148R). Resistant virus was also observed at RAL concentration corresponding to 5-fold the EC_{50} (N155H), and 40-fold the EC_{50} (Q148K). Wild-type virus by population sequencing was associated with viral breakthrough for EVG and RAL at the other drug concentrations. These observed wild-type breakthroughs may be due to incomplete integration inhibition relating to the high MOI of these infections or low-levels of resistance not detected by standard population sequencing. Among the breakthrough selections with resistance mutations detected, the mutations observed corresponded to established resistance mutations for EVG and RAL.

3.3. Phenotypic analyses of site-directed mutant viruses

Mutations observed to develop during the drug selection experiments were engineered into the wild-type HIV-1 pHXB2D plasmid

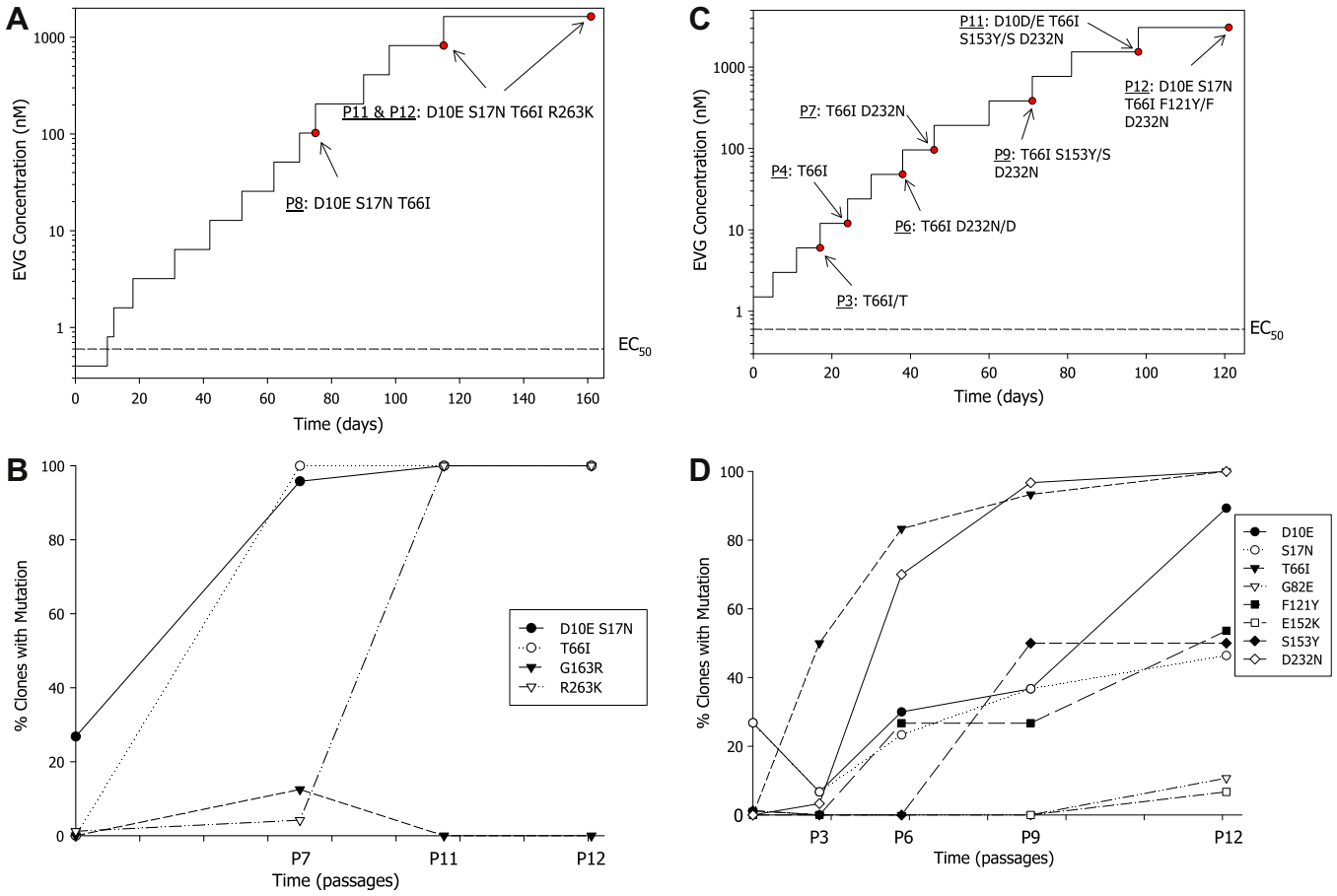

Fig. 3. HIV-1 selection time courses using EVG (panel A, replicate #1; panel C, replicate #2). Clonal sequencing analysis of the selected viral pools (24–30 clones per timepoint) is shown underneath the selection time course for each of the selections (panel B, clonal sequencing from EVG #1 selection; panel D, clonal sequencing from EVG #2 selection). Amino acid changes compared to HIV-1_{IIIB} starting material (time 0) are plotted.

Table 3
Genotypic results from the breakthrough selections.

Selecting compound[a,b]	Drug concentrations (fold over EC_{50}[c])				
	5	10	20	40	80
EVG	Wild-type	T66T/I	Wild-type	Q148R	Q148R
RAL	N155H	Wild-type	Wild-type	Q148K	Wild-type
EFV	nd	L100I D237D/N	L100I D237N	L100I	L100I V108I

nd, not done; EVG, elvitegravir; RAL, raltegravir; EFV, efavirenz.
[a] Changes in the integrase gene compared to wild-type HIV-1_{HXB2D} are shown for EVG and RAL.
[b] Changes in the RT gene compared to wild-type HIV-1_{HXB2D} are shown for EFV.
[c] The EC_{50} for EVG, RAL, and EFV against HIV-1_{HXB2D} were 1.2, 5.6, and 1 nM, respectively.

by site-directed mutagenesis in order to assess the individual phenotypic impact of specific mutations or combinations of mutations independent of other genetic changes (Table 4). Selection with M1 led to a resistant virus that carried the primary mutations H51Y and S147G, and the site-directed mutant virus carrying these two mutations showed a 144-fold decrease in susceptibility to M1. This double mutant also exhibited cross-resistance to the related compounds M4 and EVG, but no cross-resistance to RAL or the NRTI control compound TFV (fold change compared to wild-type $\leqslant$2.5). The magnitude of the phenotypic resistance for the H51Y and H51Y/S147G mutants was about 2-fold lower than the phenotypic resistance observed using the selected viral pools (Table 2, M1 P8 and P10).

Selection with M4 led to a final virus composed of the primary mutations E92G and S153F that replaced a transient virus from an earlier passage that contained T66A and S153F. Similarly as above, site-directed mutant viruses containing both sets of mutations were found to be resistant to M4 and cross-resistant to both related compounds (M1 and EVG), but remained sensitive to RAL and TFV. Interestingly, the level of resistance to M4 for the E92G/S153F double mutant was quite reduced compared to the selected viral pools (8-fold compared to 115-fold above wild-type, respectively; Table 2 M4 P9), and the double mutant that was shown to be transient during the selection (T66A/S153F) showed a higher level of phenotypic resistance to M4 than the E92G/S153F double mutant that replaced it by the end of the selection (19.3-fold versus 8-fold above wild-type).

The first selection experiment using EVG led to a double mutant containing T66I and R263K, and phenotypic analyses of the recombinant T66I/R263K double mutant confirmed the presence of

Table 4
Phenotypic susceptibilities of recombinant molecular clones.

Selection experiments and associated site-directed mutant viruses	EC_{50} fold change compared to wild-type[a,b]				
	M1	M4	EVG	RAL	TFV
M1 selection					
H51Y	17.8	0.8	2.9	1.2	1.5
S147G	6.8	2.7	9.5	1.2	1.6
H51Y S147G	144	12.9	33	2.1	2.5
M4 selection					
S153F	3.4	2.2	5.2	1.9	2.4
T66A	28.8	14.1	33.1	3.8	1.8
T66A S153F	29.4	19.3	54.1	1	1.7
E92G	22.1	6.5	38.4	1.7	1.9
E92G S153F	15.5	8	30.1	1.4	1.8
EVG selection #1					
T66I[c]	23.1	10.7	14.5	1.3	1
R263K	18.1	3.3	6.3	1.4	1.2
T66I R263K	297	58.3	105	1	0.5
EVG selection #2					
F121Y	19.1	12.5	11.8	7.2	1
S153Y	2.1	1.6	4.9	1.7	1.1
T66I F121Y	41.3	22.6	37.2	10.2	0.6
T66I S153Y	43.7	24.8	41.3	0.9	0.6
T66K	–	–	39.9	19.1	1.2
RAL selection					
Q148R[d]	–	–	109	37.6	0.7
RAL breakthrough selections					
N155H	–	–	41.4	23.8	1.2
Q148K	–	–	49.6	26.1	0.7

M1, metabolite 1; M4, metabolite 4; EVG, elvitegravir; RAL, raltegravir; TFV, tenofovir; '–', not determined.
[a] Wild-Type HIV-1_{HXB2D} EC_{50} values were 12.5, 10.5, 1.2, 5.6 nM, and 3.6 μM for M1, M4, EVG, RAL, and TFV, respectively.
[b] Fold change values ⩽2.5 reflect assay variation. All fold change values >2.5-fold demonstrated a statistically significant difference compared to wild-type using the student *t*-test ($p < 0.01$).
[c] The T66I mutation was also observed in the EVG selection #2 and in the breakthrough selections.
[d] The Q148R mutation was also observed in the breakthrough selections using EVG.

resistance to EVG (105-fold above wild-type), as well as high-level cross-resistance to the related compounds M1 and M4 (297- and 58-fold above wild-type, respectively). No cross-resistance to RAL was observed, underlining the specificity of the T66I mutation to EVG. The control compound TFV showed near wild-type levels of susceptibility to these mutants. The second selection experiment using EVG led to combinations of the mutants T66I/F121Y and T66I/S153Y, and phenotypic analyses of site-directed mutants containing these two sets of mutations showed a similar level of resistance to EVG (both near 40-fold above wild-type; Table 4). Phenotypic resistance to M1 was very similar to that of EVG (near 40-fold above wild-type for both T66I/F121Y and T66I/S153Y) and was about 2-fold lower for M4. Phenotypic cross-resistance to RAL was observed in the mutants containing the F121Y mutation (7.2- and 10.2-fold above wild type; Table 4), as well as for the T66K mutant which was observed in one clone at passage 6.

The Q148R mutant was observed in the RAL dose escalation selection experiment as well as in the EVG breakthrough selection, and was associated with high phenotypic resistance to both compounds (37.6- and 109-fold for RAL and EVG, respectively). The mutants that were observed specifically in the RAL breakthrough selection experiments (N155H and Q148K) gave rise to phenotypic resistance to both RAL and EVG (near 25-fold for both mutants for RAL, and 40–50-fold for both mutants for EVG).

4. Discussion

We have conducted a series of resistance selection experiments with the aim of gaining further insight into the potential development of resistance against the strand transfer integrase inhibitors RAL and EVG, as well as for the two predominant metabolites of EVG M1 and M4.

The selection experiment using the EVG metabolite M1 (elvitegravir hydroxide) led to a virus containing the mutations H51Y and S147G that was highly resistant to M1 and exhibited cross-resistance to EVG. These mutations were observed previously in EVG resistance selection experiments in association with other mutations such as E92Q (Shimura et al., 2008), and have been observed clinically in some patients failing EVG therapy, also in association with other resistance mutations (Waters et al., 2009). Therefore, the presence of these mutations upon selection with an EVG-related compound is not unexpected and does not constitute a new pattern of resistance to EVG. The mutation V281M that was present at the end of the selection with M1 is found as a low-level polymorphism in integrase treatment-naïve subjects (Ceccherini-Silberstein et al., 2010; Lataillade et al., 2007; Low et al., 2009), and is unlikely to play a role in resistance to EVG as the phenotypic resistance measured for the selected virus containing H51Y, S147G, and V281M (present at >80% based on clonal sequencing) was very similar to the phenotypic resistance measured with the site-directed mutant virus containing only H51Y and S147G (28-fold compared to 33-fold from wild-type, respectively). Interestingly, the phenotypic resistance observed for the double mutant (H51Y/S147G) is nearly equivalent to the product of the fold changes observed for each single mutant (H51Y and S147G alone) for EVG and M1, suggesting that these two mutations may have a synergistic effect on resistance to EVG and M1.

Elvitegravir breakthrough resistance selections at low EVG concentration (10× EC_{50}) led to a virus containing the T66I mutation, while breakthrough selections at higher EVG concentrations (40× EC_{50} and 80× EC_{50}) led to viruses containing the Q148R mutation. Mutations at T66 (T66I/A/K) and Q148 (Q148R/H/K) have been described previously (Goethals et al., 2008; McColl et al., 2007; Shimura et al., 2008; Waters et al., 2009) as resistance mutations

to EVG. A substitution at position T66 (T66I or A) was found to be the most prevalent resistance mutation in patients failing while receiving an EVG-containing regimen in the phase 3 clinical trial of EVG in treatment-experienced patients (Molina et al., 2011). In contrast, substitutions at T66 were not as commonly found as E92Q, Q148R/K/H, or N155H upon EVG treatment failure in an earlier phase 2 trial of EVG (McColl et al., 2007; Waters et al., 2009) where subjects were followed up for a longer period of time while experiencing virologic failure due to limited treatment options. As the clinical data suggest, the presence of mutations at residue T66 appears to represent an earlier step in the development of integrase resistance, while other mutations such as E92Q, Q148R/K/H, or N155H are representative of more advanced EVG resistance. Consequently, the results of the EVG breakthrough selections appear to recapitulate the clinical observations. Transition from a T66 resistance mutation pattern (T66A) towards an E92 resistance mutation pattern (E92G) was also observed in the resistance selection for the EVG-related metabolite M4 and was associated with increased phenotypic resistance to EVG in the viral supernatant analysis.

Two EVG dose-escalation resistance selection experiments led to the development of the T66I resistance mutation in both cases, suggesting that the starting EVG concentration (either $1\times$ EC_{50} or $2\times$ EC_{50}) had little effect on the primary mutation pattern of the resulting virus, even though the mutations associated with T66I in both cases were different (R263K or F121Y/S153Y, respectively). These secondary mutations, which were associated with increased phenotypic resistance in both cases, may reflect the stochastic nature of resistance selection experiments. All three secondary integrase mutations are >99% conserved in integrase inhibitor treatment-naïve subjects (Ceccherini-Silberstein et al., 2010; Low et al., 2009), and both F121Y and S153Y were found independently in resistance selection experiments conducted with other integrase inhibitor compounds containing a diketo acid moiety (Shimura and Kodama, 2009; Witmer and Danovich, 2009). Phenotypic data from these mutants have shown that high levels of EVG resistance can be achieved when combining the T66I mutation with these secondary integrase mutations. Interestingly, no cross-resistance to RAL was associated with T66I, but cross-resistance to RAL was noted for both the T66A and T66K mutants, as well as the F121Y mutant.

Several mutations that have been found repeatedly in our in vitro selection experiments are unlikely to play a role in EVG resistance as they have been reported as polymorphic sites by several groups (Ceccherini-Silberstein et al., 2010; Lataillade et al., 2007; Low et al., 2009). Specifically, D10E and S17N were present in >20% of the clones analyzed from the wild-type starting material HIV-1_{IIIB} (time 0, Figs. 2B and D and 3B and D), and the other mutation, D232N, corresponds to the consensus amino acid for the wild-type strain HIV-1_{HXB2D} and is not associated with phenotypic resistance. The presence (or absence) of these mutations in any of the selected viruses is likely a reflection of the stochastic nature and founder effects associated with in vitro selection experiments, rather than associated with resistance to the compounds tested.

In conclusion, we have shown through a series of resistance selection experiments that the predominant metabolites of EVG M1 and M4 led to the development of resistance mutations that had been observed previously in vivo and/or in vitro in association with EVG (H51Y, T66A, T66I, E92G, S147G), as well as a novel S153F mutation. Additional EVG selection experiments led to the development of the F121Y and S153Y mutations which were previously associated with other diketo acid strand transfer inhibitors but have not been previously reported to be associated with EVG. A novel mutation R263K was also identified in these experiments. Among these mutations not previously associated with EVG R263K and S153F each developed in one EVG-treated subject during clinical studies of EVG ((McColl et al., 2007), unpublished observations). Overall, the in vitro studies presented here demonstrate that the resistance profile of the M1 and M4 metabolites of EVG which are present at only low levels in vivo have a resistance profile that overlaps with that of the parent molecule EVG. Moreover, available clinical data indicate that the resistance profile of EVG in vivo is defined by that of the active drug, elvitegravir.

Acknowledgments

The authors wish to thank Michael Abram for his critical review of the manuscript, as well as Katyna Borroto-Esoda and Christian Callebaut for their scientific insight throughout these studies, and Heidi Fisher for her technical assistance.

References

Ceccherini-Silberstein, F., Malet, I., Fabeni, L., Dimonte, S., Svicher, V., D'Arrigo, R., Artese, A., Costa, G., Bono, S., Alcaro, S., Monforte, A., Katlama, C., Calvez, V., Antinori, A., Marcelin, A.G., Perno, C.F., 2010. Specific HIV-1 integrase polymorphisms change their prevalence in untreated versus antiretroviral-treated HIV-1-infected patients, all naive to integrase inhibitors. J. Antimicrob. Chemother. 65, 2305–2318.

Cherepanov, P., Ambrosio, A.L., Rahman, S., Ellenberger, T., Engelman, A., 2005. Structural basis for the recognition between HIV-1 integrase and transcriptional coactivator p75. Proc. Natl. Acad. Sci. USA 102, 17308–17313.

Cherepanov, P., Maertens, G., Proost, P., Devreese, B., Van Beeumen, J., Engelborghs, Y., De Clercq, E., Debyser, Z., 2003. HIV-1 integrase forms stable tetramers and associates with LEDGF/p75 protein in human cells. J. Biol. Chem. 278, 372–381.

Cooper, D.A., Steigbigel, R.T., Gatell, J., Rockstroh, J., Katlama, C., Yeni, P., Lazzarin, A., Clotet, B., Kumar, P., Eron, J.E., Schechter, M., Markowitz, M., Loutfy, M.R., Lennox, J.L., Zhao, J., Chen, J., Ryan, D.M., Rhodes, R.R., Killar, J.A., Gilde, L.R., Strohmaier, K.M., Meibohm, A.R., Miller, M.D., Hazuda, D.J., Nessly, M.L., DiNubile, M.J., Isaacs, R.D., Teppler, H., Nguyen, B., 2008. Subgroup and resistance analyses of raltegravir for resistance HIV-1 Infection. N. Engl. J. Med. 359, 355–365.

Dorr, P., Westby, M., Dobbs, S., Griffin, P., Irvine, B., Macartney, M., Mori, J., Rickett, G., Smith-Burchnell, C., Napier, C., Webster, R., Armour, D., Price, D., Stammen, B., Wood, A., Perros, M., 2005. Maraviroc (UK-427, 857), a potent, orally bioavailable, and selective small-molecule inhibitor of chemokine receptor CCR5 with broad-spectrum anti-human immunodeficiency virus type 1 activity. Antimicrob. Agents Chemother. 49, 4721–4732.

Fransen, S., Gupta, S., Danovich, R., Hazuda, D., Miller, M., Witmer, M., Petropoulos, C.J., Huang, W., 2009. Loss of raltegravir susceptibility by human immunodeficiency virus type 1 is conferred via multiple nonoverlapping genetic pathways. J. Virol. 83, 11440–11446.

Goethals, O., Clayton, R., Van Ginderen, M., Vereycken, I., Wagemans, E., Geluykens, P., Dockx, K., Strijbos, R., Smits, V., Vos, A., Meersseman, G., Jochmans, D., Vermeire, K., Schols, D., Hallenberger, S., Hertogs, K., 2008. Resistance mutations in human immunodeficiency virus type 1 integrase selected with elvitegravir confer reduced susceptibility to a wide range of integrase inhibitors. J. Virol. 82, 10366–10374.

Johnson, V.A., Brun-Vezinet, F., Clotet, B., Gunthard, H.F., Kuritzkes, D.R., Pillay, D., Schapiro, J.M., Richman, D.D., 2010. Update of the drug resistance mutations in HIV-1: December 2010. Top. HIV Med. 18, 156–163.

Kilby, J.M., Hopkins, S., Venetta, T.M., DiMassimo, B., Cloud, G.A., Lee, J.Y., Alldredge, L., Hunter, E., Lambert, D., Bolognesi, D., Matthews, T., Johnson, M.R., Nowak, M.A., Shaw, G.M., Saag, M.S., 1998. Potent suppression of HIV-1 replication in humans by T-20, a peptide inhibitor of gp41-mediated virus entry. Nat. Med. 4, 1302–1307.

Kobayashi, M., Yoshinaga, T., Seki, T., Wakasa-Morimoto, C., Brown, K.W., Ferris, R., Foster, S.A., Hazen, R.J., Miki, S., Suyama-Kagitani, A., Kawauchi-Miki, S., Taishi, T., Kawasuji, T., Johns, B.A., Underwood, M.R., Garvey, E.P., Sato, A., Fujiwara, T., 2011. In Vitro antiretroviral properties of S/GSK1349572, a next-generation HIV integrase inhibitor. Antimicrob. Agents Chemother. 55, 813–821.

Lataillade, M., Chiarella, J., Kozal, M.J., 2007. Natural polymorphism of the HIV-1 integrase gene and mutations associated with integrase inhibitor resistance. Antivir. Ther. 12, 563–570.

Low, A., Prada, N., Topper, M., Vaida, F., Castor, D., Mohri, H., Hazuda, D., Muesing, M., Markowitz, M., 2009. Natural polymorphisms of human immunodeficiency virus type 1 integrase and inherent susceptibilities to a panel of integrase inhibitors. Antimicrob. Agents Chemother. 53, 4275–4282.

Maertens, G., Cherepanov, P., Pluymers, W., Busschots, K., De Clercq, E., Debyser, Z., Engelborghs, Y., 2003. LEDGF/p75 is essential for nuclear and chromosomal targeting of HIV-1 integrase in human cells. J. Biol. Chem. 278, 33528–33539.

Malet, I., Delelis, O., Valantin, M.A., Montes, B., Soulie, C., Wirden, M., Tchertanov, L., Peytavin, G., Reynes, J., Mouscadet, J.F., Katlama, C., Calvez, V., Marcelin, A.G., 2008. Mutations associated with failure of raltegravir treatment affect integrase sensitivity to the inhibitor in vitro. Antimicrob. Agents Chemother. 52, 1351–1358.

Marchand, C., Maddali, K., Metifiot, M., Pommier, Y., 2009. HIV-1 IN inhibitors: 2010 update and perspectives. Curr. Top. Med. Chem. 9, 1016–1037.

Marinello, J., Marchand, C., Mott, B.T., Bain, A., Thomas, C.J., Pommier, Y., 2008. Comparison of raltegravir and elvitegravir on HIV-1 integrase catalytic reactions and on a series of drug-resistant integrase mutants. Biochemistry 47, 9345–9354.

McColl, D.J., Fransen, S., Gupta, S., Parkin, N., Margot, N., Ledford, R., Chen, J., Chuck, S., Cheng, A.K., Miller, M.D., 2007. Resistance and cross-resistance to first generation integrase inhibitors: Insights from a phase 2 study of Elvitegravir (GS-9137) [abstract number 9], 16th International HIV Drug Resistance Workshop. Bridgetown, Barbados.

Molina, J.M., Lamarca, A., Andrade-Villanueva, J., Clotet, B., Clumeck, N., Liu, Y.P., Zhong, L., Margot, N., Cheng, A.K., Chuck, S.L., 2011. Efficacy and safety of once daily elvitegravir versus twice daily raltegravir in treatment-experienced patients with HIV-1 receiving a ritonavir-boosted protease inhibitor: randomised, double-blind, phase 3, non-inferiority study. Lancet Infect Dis.

Pommier, Y., Johnson, A.A., Marchand, C., 2005. Integrase inhibitors to treat HIV/AIDS. Nat. Rev. Drug Discov. 4, 236–248.

Ramanathan, S., Wright, M., West, S., Kearney, B.P., 2007. Pharmacokinetics, metabolism and excretion of ritonavir-boosted GS-9137 (elvitegravir) [poster number 30], 8th International Workshop on Clinical Pharmacology of HIV Therapy, Budapest, Hungary.

Shimura, K., Kodama, E., Sakagami, Y., Matsuzaki, Y., Watanabe, W., Yamataka, K., Watanabe, Y., Ohata, Y., Doi, S., Sato, M., Kano, M., Ikeda, S., Matsuoka, M., 2008. Broad antiretroviral activity and resistance profile of the novel human immunodeficiency virus integrase inhibitor elvitegravir (JTK-303/GS-9137). J. Virol. 82, 764–774.

Shimura, K., Kodama, E.N., 2009. Elvitegravir: a new HIV integrase inhibitor. Antivir. Chem. Chemother. 20, 79–85.

van Lunzen, J., Maggiolo, F., Arribas, J.R., Rakhmanova, A., Yeni, P., Young, B., Rockstroh, J.K., Almond, S., Song, I., Brothers, C., Min, S., 2011. Once daily dolutegravir (S/GSK1349572) in combination therapy in antiretroviral-naive adults with HIV: planned interim 48 week results from SPRING-1, a dose-ranging, randomised, phase 2b trial. Lancet Infect Dis.

Waters, J.M., Margot, N., Hluhanich, R., Svarovskaia, J., Harris, J., Borroto-Esoda, K., Miller, M.D., McColl, D.J., 2009. Evolution of Resistance to the HIV Integrase Inhibitor (INI) Elvitegravir Can Involve Genotypic Switching Among Primary INI Resistance Patterns [Poster P116], XVIII International HIV Drug Resistance Workshop, Fort Myers, Florida.

Witmer, M., Danovich, R., 2009. Selection and analysis of HIV-1 integrase strand transfer inhibitor resistant mutant viruses. Methods (San Diego, Calif) 47, 277–282.

Yoder, K.E., Bushman, F.D., 2000. Repair of gaps in retroviral DNA integration intermediates. J. Virol. 74, 11191–11200.

Yoder, K.E., Espeseth, A., Wang, X.H., Fang, Q., Russo, M.T., Lloyd, R.S., Hazuda, D., Sobol, R.W., Fishel, R., 2011. The base excision repair pathway is required for efficient lentivirus integration. PLoS One 6, e17862.